Analytical Studies on Reinforced Concrete Columns subjected to Bi-axial Bending

Tomohiro NAKANO*, Tada-aki TANABE**

* M.of Eng., Dept. of Civil Eng., Nagoya University, 1, Furo-cho, Nagoya-shi, Aichi 464-8603
** Dr.of Eng., Professor, Dept. of Civil Eng., Nagoya University, 1, Furo-cho, Nagoya-shi, Aichi 464-8603

Beams are typically subjected to uniaxial bending, whereas columns are subjected to bi-axial bending with axial force. In general, under bi-axial bending, the degradation of resisting force along the principal axis in case bi-axial bending exists becomes larger in comparison with the one of uni-axial bending. In this paper, we applied flexibility method, which is force-based formulation, to nonlinear static and dynamic analysis for RC columns. In addition to this, analytical simulations and discussions for bi-axial bending are obtained.

Key Words: Bi-Axial Bending, Fiber Model, Flexibility Method

1.Introduction

The frame member that receives the earthquake or/and eccentric loading with permanent eccentric axial load is subjected to bi-axial bending and is forced into a state of non-symmetric stress condition. As is well known the degradation of resisting force along the principal axis in case bi-axial bending exists becomes larger in comparison with the one of uni-axial bending [1),2)]. Therefore it is insufficient for RC members under bi-axial bending to apply superposing in-plane behavior. For that reason, it may be insufficient to consider seismic response of structures by simply superposing the stress conditions of two principal directions that are obtained independently [3)].

Furthermore, there are many public structures, which are always subjected to bi-axial bending for their configuration. Many such structures must be analyzed as total structure system, however the displacement based beam element needs many degree-of-freedoms for this purpose [4)].

This study aims at explication of the behavior of RC members subjected to bi-axial bending under static and dynamic loading by combination of the three-dimensional fiber-model [5)] and the flexibility method [6)] which makes degree-of-freedoms degrade.

In this paper, we applied fiber-model and flexibility method, which is force-based formulation, to nonlinear analysis for RC columns, and an analytical simulation for bi-axial bending is obtained. In addition to these analyses, we investigated the differences between the behaviors with or without bi-axial bending and various seismic waves, systematically.

2. Element Formulations [7)]

2.1 Displacement-based element formulation

In the displacement-based element formulation, the basic concept is to express the displacement field $\mathbf{u}(x)$ as a function of the displacement interpolation function $N_D(x)$ and nodal displacement $\mathbf{q}$.

$$\mathbf{u}(x) = N_D(x) \cdot \mathbf{q} \tag{1}$$

Here, $N_D(x)$ for axial displacement is assumed to be a linear function and $N_D(x)$ for flexure to be a cubic. To translate $\mathbf{u}(x)$ into the strain $\varepsilon(x)$, let differentiate $N_D(x)$

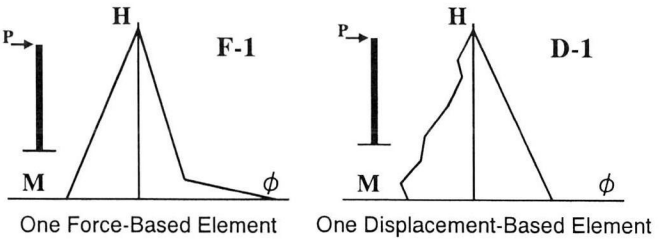

Fig.1 Differences between Force- and Displacement-based Element

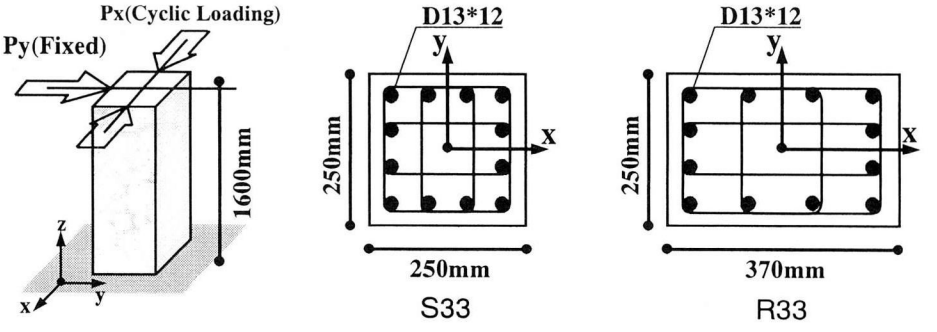

Fig.2 Summary of specimens

and we get

$$\varepsilon(x) = B(x) \cdot q \tag{2}$$

where $B(x)$ are the strain-displacement operator containing the first and second derivatives of $N_D(x)$. Now, introducing the section stiffness in the element $k(x)$, section force vector can be expressed as $S(x)=k(x)\ \varepsilon\ (x)$.

The principle of virtual displacements yields the element stiffness matrix K and element forces Q can be obtained as follows.

$$K = \int_0^L B^T(x)\, k(x)\, B(x)\, dx \tag{3}$$

$$Q = \int_0^L B^T(x)\, S(x)\, dx \tag{4}$$

In these formulations, the equilibrium of forces is expressed in Eq.4 as the relationship between the nodal forces Q and internal forces $S(x)$. Therefore these formulation must be used so long as curvature is linear. If the curvature is not linear distribution, we have to make the member divide finer elements.

2.2 Force-based element formulation

In the force-based element formulation, the basic concept is to express the force field $S(x)$ as a function of the force interpolation function $N_F(x)$ and nodal forces Q

$$S(x) = N_F(x) \cdot Q \tag{5}$$

where $N_F(x)$ are the interpolation functions. For axial forces, $N_F(x)$ is constant and for flexure, $N_F(x)$ is linear function of x. Introducing the section flexibility $f(x)$ yields the relation

$$\varepsilon(x) = f(x) \cdot S(x) \tag{6}$$

Application of the principle of virtual forces yields the element flexibility matrix

$$F = \int_0^L N_F^T(x)\, f(x)\, N_F(x)\, dx \tag{7}$$

In the force-based formulation, the exact force interpolation function can be determined. Therefore the flexibility matrix of Eq.7 is exact.

These formulations are based on the equilibrium of forces. Therefore flexibility method can estimate the accurate moment and curvature distribution by just one element so long as force distribution is linear, which are usual cases in real column structures. The differences of internal moment and curvature distributions between force- and displacement-based element are shown in **Fig.1**. The special feature of flexibility method is 3-step algorithm, that is, structure-, element- and section-state determination processes. Details of these algorithms are shown in Ref. 4),6),8).

3. Analyses of the RC Columns Tests subjected to Bi-axial Bending [2),9)]

3.1 Test specimens

To show the availability of flexibility method, the

Table 1 Material Properties

CONCRETE	
Initial Modulus	21.00 [GPa]
Strain at Max. Stress	0.0025
Compressive Strength	31.40 [MPa]
Tension Strength	2.50 [MPa]
STEEL	
Initial Modulus	184.20 [GPa]
Yield Strength	371.40 [MPa]

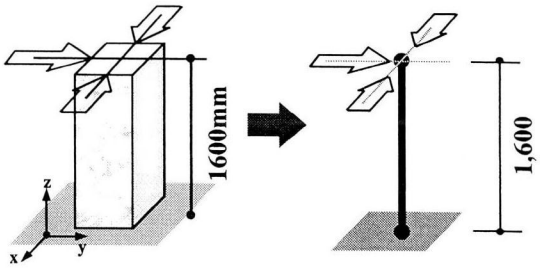

Fig.3 Modeling of the specimen

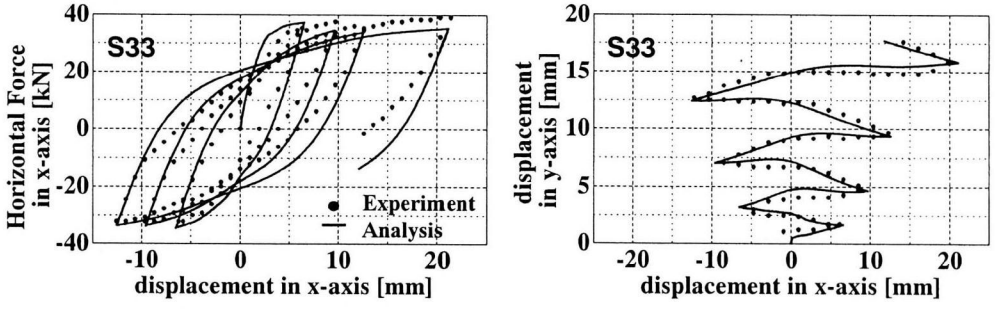

Fig.4 Comparison of load-deflection curve in x-direction and deflection of x-dir vs. y-dir (S33)

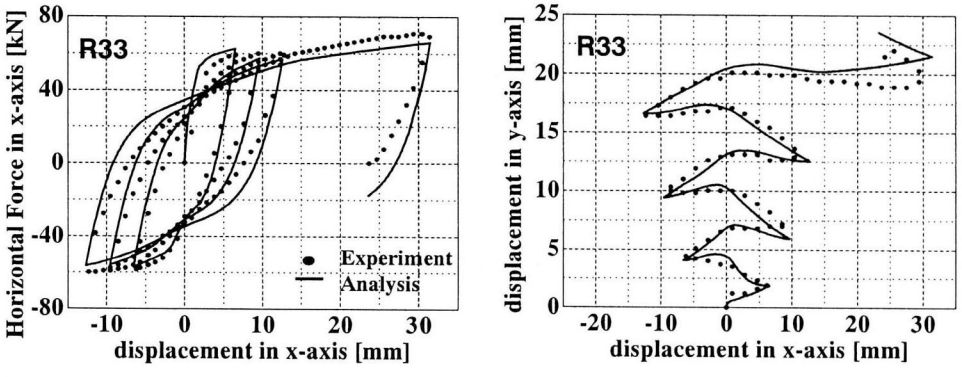

Fig.5 Comparison of load-deflection curve in x-direction and deflection of x-dir vs. y-dir (R33)

cyclic analyses under bi-axial bending which were tested by Sato et al. were carried out in this paper. Summary of the specimens is shown in **Fig.2**. These specimens have a square section (S33: 250mm*250mm) and a rectangular section (R33: 370mm*250mm), respectively. In these experiments, the cyclic horizontal displacement in the x-direction and the y-directional horizontal force applied constantly to column specimen. Material properties are shown in **Table 1**.

3.2 Analysis model and analytical results

In case of the above-mentioned specimen, the RC column can be modeled by one element in flexibility method (**Fig.3**). To analyze these specimens, we take fiber-model to obtain section stiffness and hysteresis. In fiber-model, constitutive relations of concrete and steel were Darwin-Pecknold model [10] and Menegotto-Pinto model [11], respectively.

Analytical results and experimental results are shown in **Figs.4-5**. In **Fig.4**, Load-displacement curve in x-direction of S33 and displacement of x-direction vs. that of y-direction of S33 are shown. Similarly, those of R33 are shown in **Fig.5**.

These P-D relationships have a little differences in hysteresis range, however the tendency of experimental results and analysis are almost same. Furthermore, the phenomena that the deflection of the y-direction gets larger though the horizontal force in the y-direction keeps constant are represented in both specimens. As a whole, these results show that the analysis is reasonable.

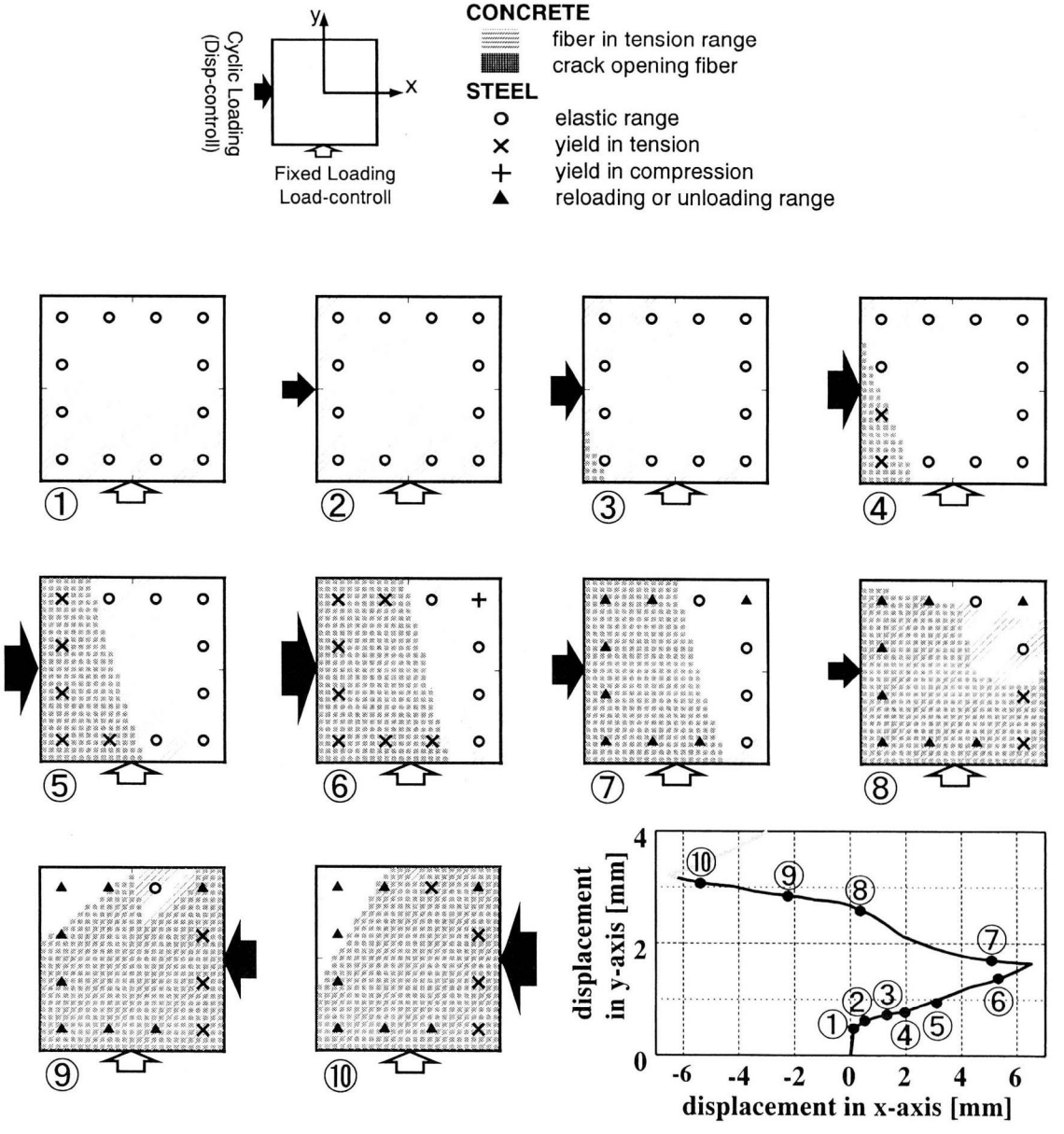

Fig.6 Damage progress of the section at the bottom of column

3.3 Mechanisms of RC column behavior under bi-axial bending

To explain the mechanisms of bi-axial bending of RC column, especially increment of deflection of y-direction in **Fig.4**, the processes of concrete cracking and the state of steels are shown in **Fig.6**. The numbers of **Fig.6** are corresponding to that of Dx-Dy relationship in **Fig.6**, respectively. Moreover, the black arrows mean the displacement given in x-axis conceptually. In this figure, we judge the crack opening when the concrete fiber is in the tension-strain and the tension-stress is zero.

From **Fig.6**, we can get the following explanation.

1) In ①-③ in **Fig.6**, all steels do not yield. At this moment, the slope of neutral axis changes according to the ratio between the horizontal force in x-direction and that of z-direction. However, the stiffness in y-direction degrades because crack occurs due to the force in x-direction in ③. This is the cause of occurrence of displacement in y-direction progress.
2) In ④-⑥, steels yield in tension by the increment of forces in x-direction. As steel yielding, the stiffness in y-direction degrades suddenly although the force in y-direction keeps constant. These phenomena make the displacement in y-direction increase.
3) In ⑧ in **Fig.6**, although the displacement in x-axis is positive, two steels in lower-right side yields in tension. In these steels, there occurs tension stress by increasing of the displacement in y-direction.
4) In ⑨-⑩, cracking range in concrete and steel strain

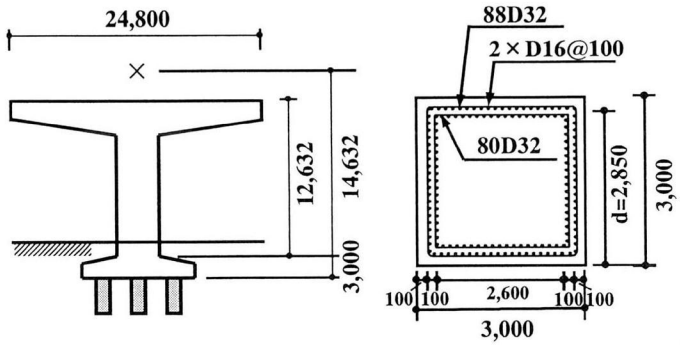

Fig.7 Structure for analysis

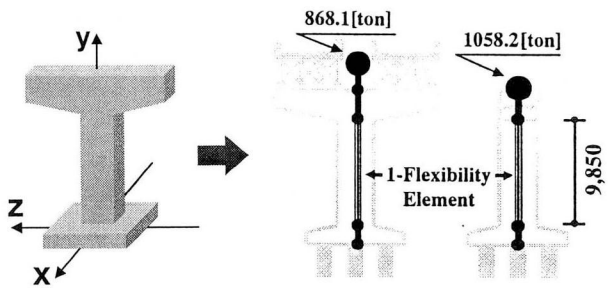

Fig.8 Modeling of the pier

Table 2 Material Properties

CORE CONCRETE	
Initial Modulus **Ec**	25.00 [GPa]
Compressive Strength σc	28.80 [MPa]
Strain at Max. Stress εc	0.0028
Tension Strength	2.88[Mpa]
Softening Slope **Edes**	-5178.0
COVER CONCRETE	
Initial Modulus **Ec**	25.00 [GPa]
Compressive Strength σc	27.50 [MPa]
Strain at Max. Stress εc	0.0020
Tension Strength	2.75[Mpa]
Softening Slope **Edes**	-13775.0
STEEL (SD-30)	
Initial Modulus	195.20 [GPa]
Yield Strength	328.00 [MPa]

① $\sigma = E_c\varepsilon_c\left\{1-\frac{1}{n}\left(\frac{\varepsilon}{\varepsilon_c}\right)^{n-1}\right\}$

$n = \frac{E_c\varepsilon_c}{E_c\varepsilon_c - \sigma_c}$

② Parabola

③ $\sigma = \sigma_c + E_{des}(\varepsilon - \varepsilon_c)$

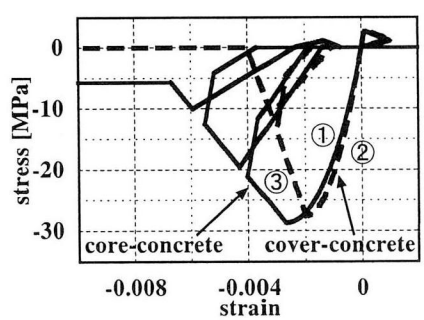

a) concrete

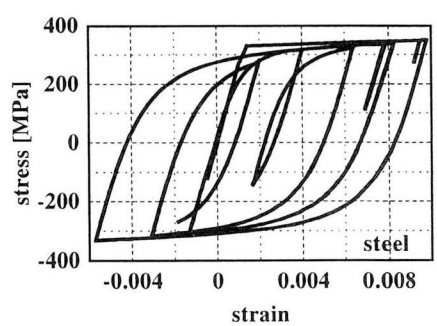

b) steel

Fig.9 Constitutive Relations

increase. Therefore the stiffness in y-direction decrease less and less.

As stated above, in bi-axial bending, damage of concrete or/and steels of one direction contribute to the deflection or resisting-force in other direction. These phenomena cannot be considered by 2-dimensional analysis and 3-dimensional analysis can explain the complex behavior as RC members under bi-axial bending.

4. Analyses of the RC Bridge Piers under 3-D Seismic Loading

4.1 Summary of the structure for analyses

To investigate the influence of the effect of bi-axial bending upon the seismic performance of the structures, 3-dimensional analyses based on flexibility method are carried out. The bridge pier for these analyses is shown in **Fig.7**. This bridge is in daily use and its piers form a line with intervals of 30.0m. Cross-section of this pier is the square of 3.0m*3.0m. Material properties are shown in **Table 2**.

4.2 Analysis model, section hysteresis and analysis patterns

For the numerical simulations of above-mentioned bridge pier, this pier is modeled in 3-dimensional beam element as shown in **Fig.8**. Generally, the analysis based on stiffness method needs to divide column into finer element. However, the algorithm of the flexibility method is based on the linearity of forces as described in chap.2. Therefore, it is possible to analyze the performance of RC structure including localization by just one element.

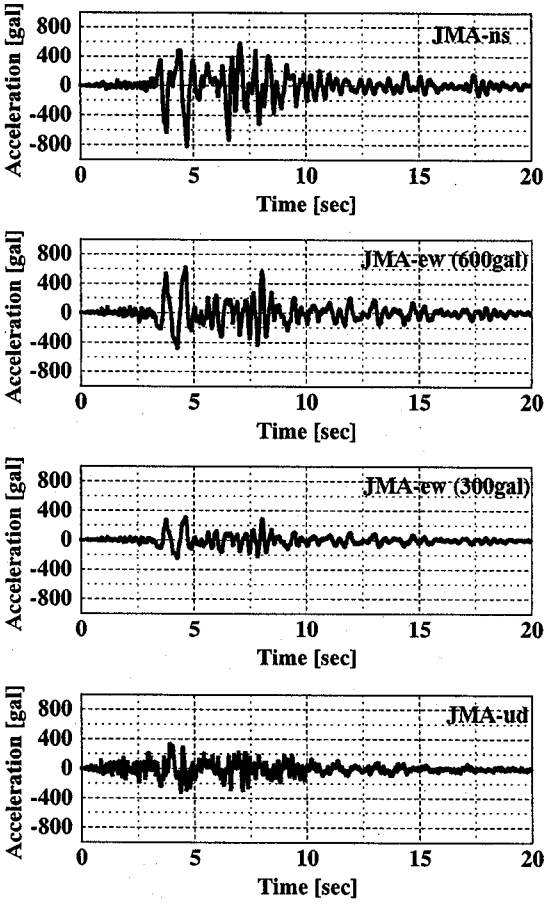

Fig.10 Input Seismic Waves (JMA)

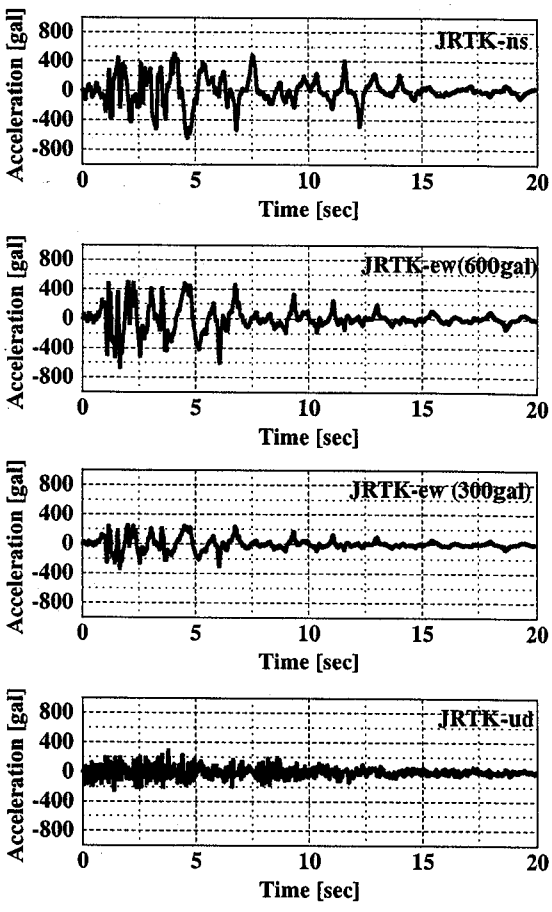

Fig.11 Input Seismic Waves (JRTK)

Table 3 Pattern of input seismic wave combination

Direction	Pattern of wave combination					
	JMA-A	JMA-B	JMA-C	JRTK-A	JRTK-B	JRTK-C
x	JMA-ns	JMA-ns	JMA-ns	JRTK-ns	JRTK-ns	JRTK-ns
z	0	JMA-ew(300)	JMA-ew(600)	0	JRTK-ew(300)	JRTK-ew(600)
y	JMA-ud	JMA-ud	JMA-ud	JRTK-ud	JRTK-ud	JRTK-ud

Consequently, the column is replaced by one flexibility element, and other elements by rigid.

Considering the height of the center of gravity of the super-structure, mass is set as **Fig.8** [12]. Besides, the bottom of the pier is fixed.

Damping matrix is assembled by the method suggested by Wilson and Penzien [13]. The damping ratios are 0.02 in non-linear flexibility element and 0.05 in rigid elements [12].

The section hysteresis is obtained by fiber-model. In fiber-model, envelope of core concrete were obtained by the model of Hoshikuma, et al. [14], and that of cover concrete by Watanabe, et al[15]. Steel constitutive relations are calculated by Menegotto-Pinto model. (**Fig.9**).

Next, the input seismic waves are the earthquake at Kobe Marine Meteorological Observatory [JMA] and JR Takatori Station [JRTK] in the Hyogo-ken-nanbu earthquake, 1995. To examine the effect of bi-axial bending, we analyze 6 patterns of wave combination, that is,

1) No wave is inputted to z-direction and NS-wave is inputted to x-direction with UD-wave (pattern JMA/JRTK-A).
2) ES-300gal-wave or ES-600gal-wave is inputted to z-direction and NS-wave is inputted to x-direction with UD-wave (pattern JMA/JRTK-B, JMA/JRTK-C).

Here, EW-300gal-wave is the half amplitude wave of EW-600gal-wave(**Figs.10-11**). Summary of analyzed wave patterns are shown in **Table 3**.

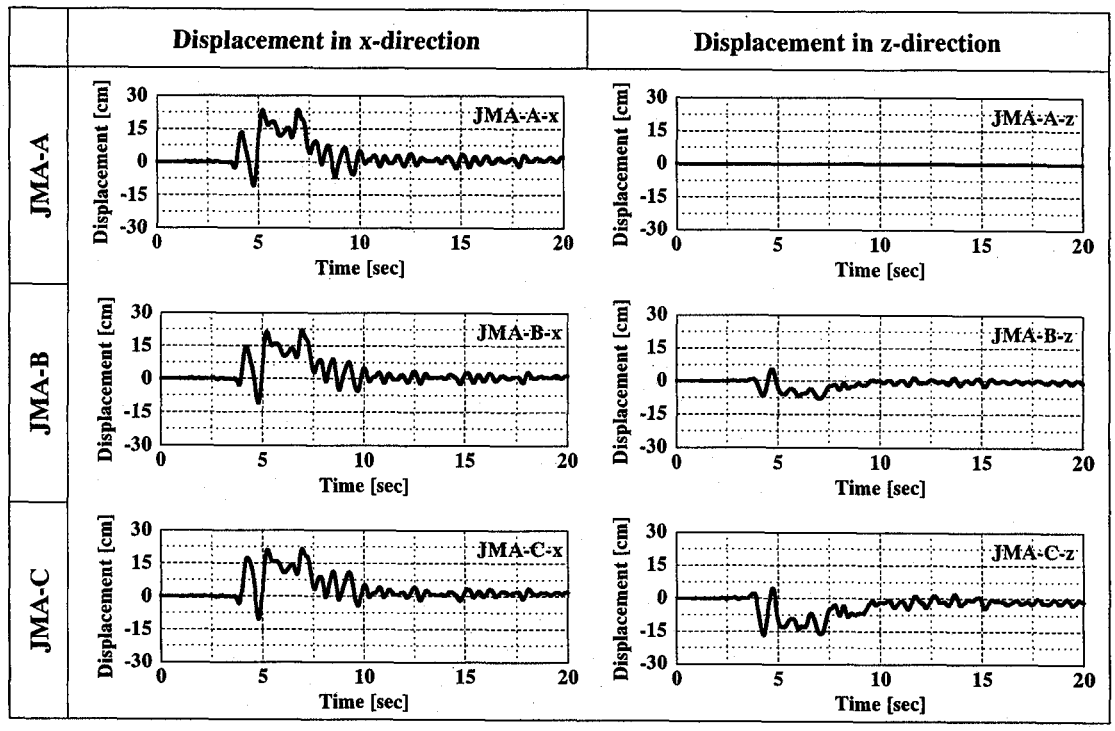

Fig.12 Displacement Response (JMA)

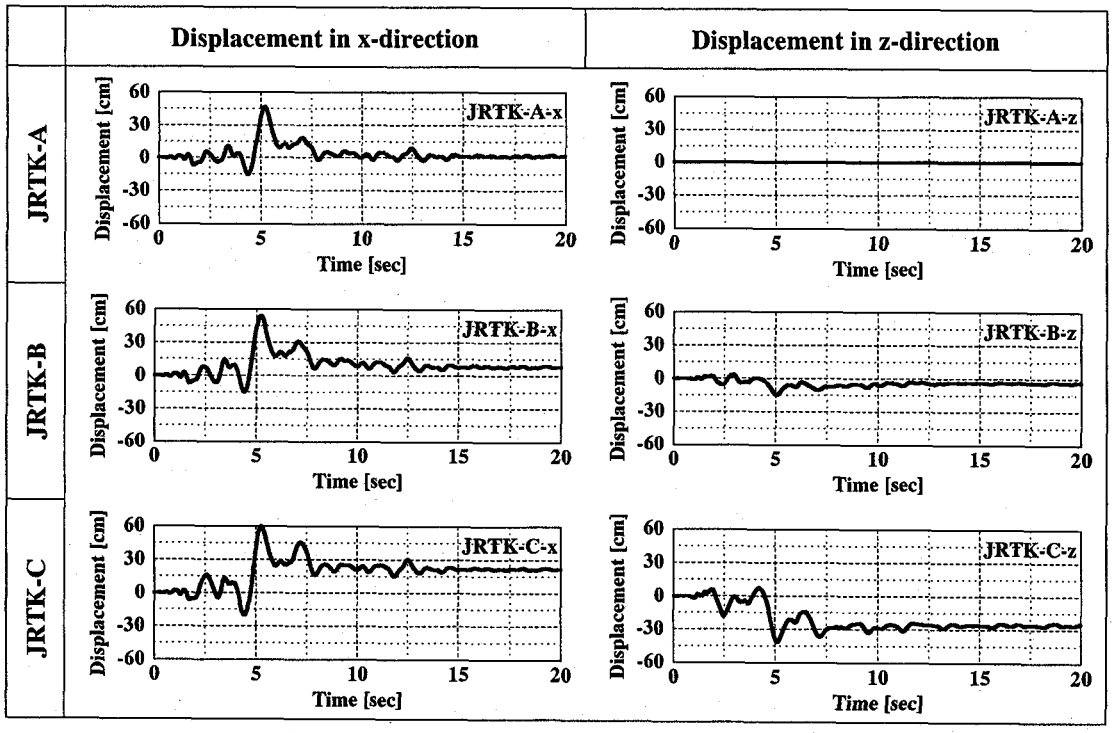

Fig.13 Displacement Response (JRTK)

4.3 Analytical results

Analytical results of pattern JMA-A,B,C are shown in **Fig.12**. According to this figure, almost no residual displacements are generated in both directions. In addition to this, displacement responses in x-direction are very similar though seismic wave in z-direction exists. Therefore, it can be said that in the case of JMA, displacement responses in x-direction in these three patterns are not influenced by the seismic wave in z-direction.

In contrast to these results, analytical results of pattern JRTK-A,B,C shown in **Fig.13** differ each other. The tendency that residual displacement increases as the seismic wave in z-direction increases. Further, the

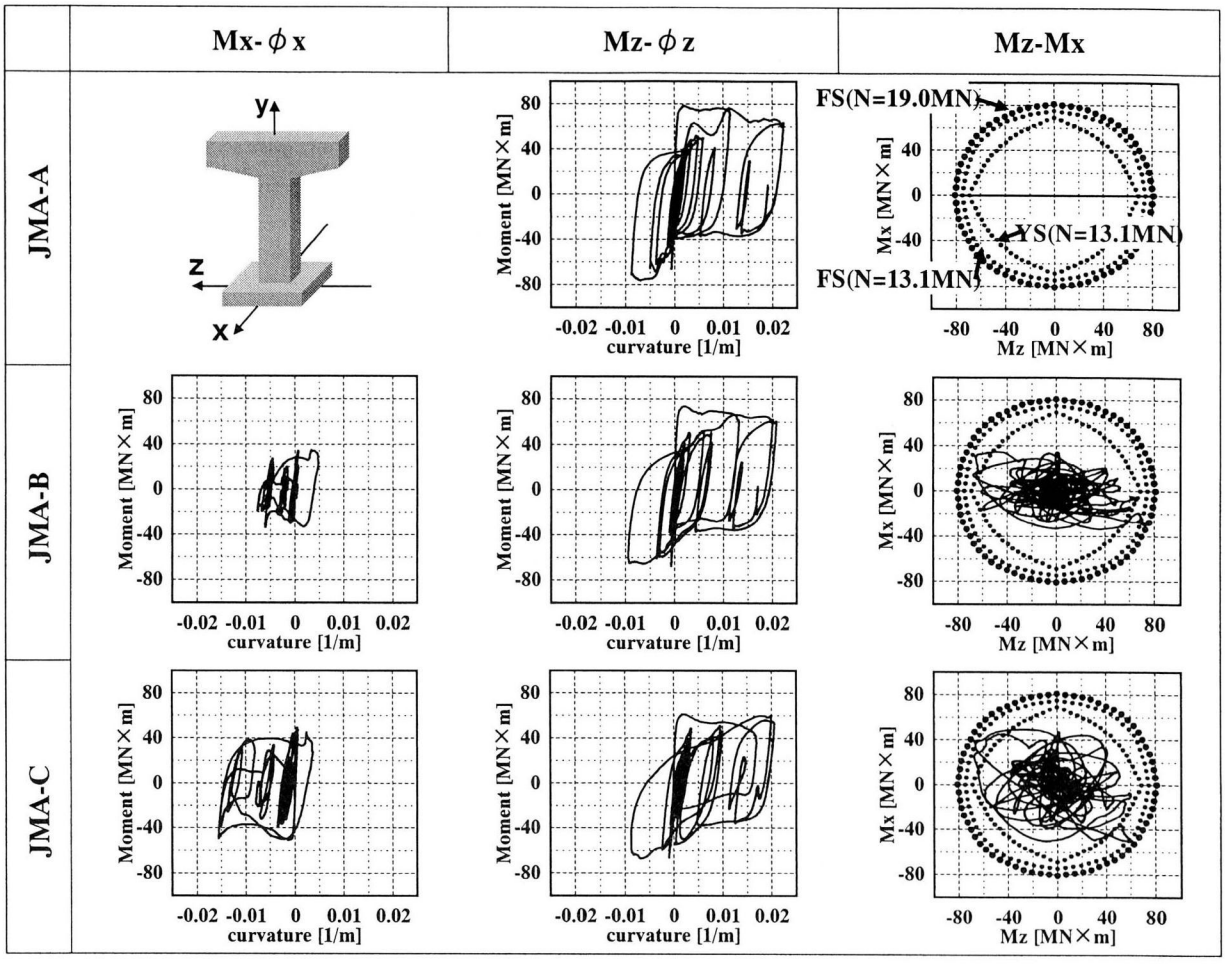

Fig.14 Section hysteresis loops (JMA)

maximum displacement responses show same trend.

These results show that the column under bi-axial bending does not always produce larger displacement response or residual displacement [3]. The reason of it will be described later.

4.4 Section hysteresis loops

The hysteresis loops at the bottom of the pier of above-mentioned analytical patterns are shown in **Figs.14-15**.

In **Fig.14-15**, pattern A shows the section hysteresis in case of NS-wave in x-direction only, B that of NS-wave in x-direction with EW-300gal-wave in z-direction, and C that of NS-wave in x-direction with EW-600gal-wave in z-direction, respectively. Mz-ϕz relations in this figure shows the tendency that the maximum moment around z-axis decrease as the input wave in z-direction increases. The differences of the maximum moment around z-axis between pattern A and C are 24%(JMA) and 23%(JRTK) of Mz of pattern A. These results show that the resisting capacity around z-axis decreases as the generation of the moment around x-axis due to the effect of bi-axial bending. Therefore it will be the risky judgement if the judgement is based on the projection of 2-dimensional analysis.

The third columns in **Figs.14-15** show the relation between moment around z-axis and that of x-axis. In these figures, FS means failure surface of the section, YS yield surface, and N means axial force. Here, failure surface is the combination of maximum moment around x-axis and that of z-axis under each moment ratio. The axial force contributed by dead load is 13.1[MN] and the maximum varying axial forces are 19.0 [MN] (JMA) and 20.1 [MN] (JRTK). All of Mz-Mx relation shows that the amplitudes of composition of moment can not cross the failure surface. Therefore, the maximum moment degradations in x-axis are caused by the degradation of projection of failure surface on x-axis.

However, there is a great difference between projection of JMA and that of JRTK. **Fig.16** shows the projection of the contact point with failure surface (JMA-C and JRTK-C). This figure indicates that the projections of 3D-failure points of JMA are close to 2D-failure points. On the other hand, the projections of 3D-failure points of JRTK are far

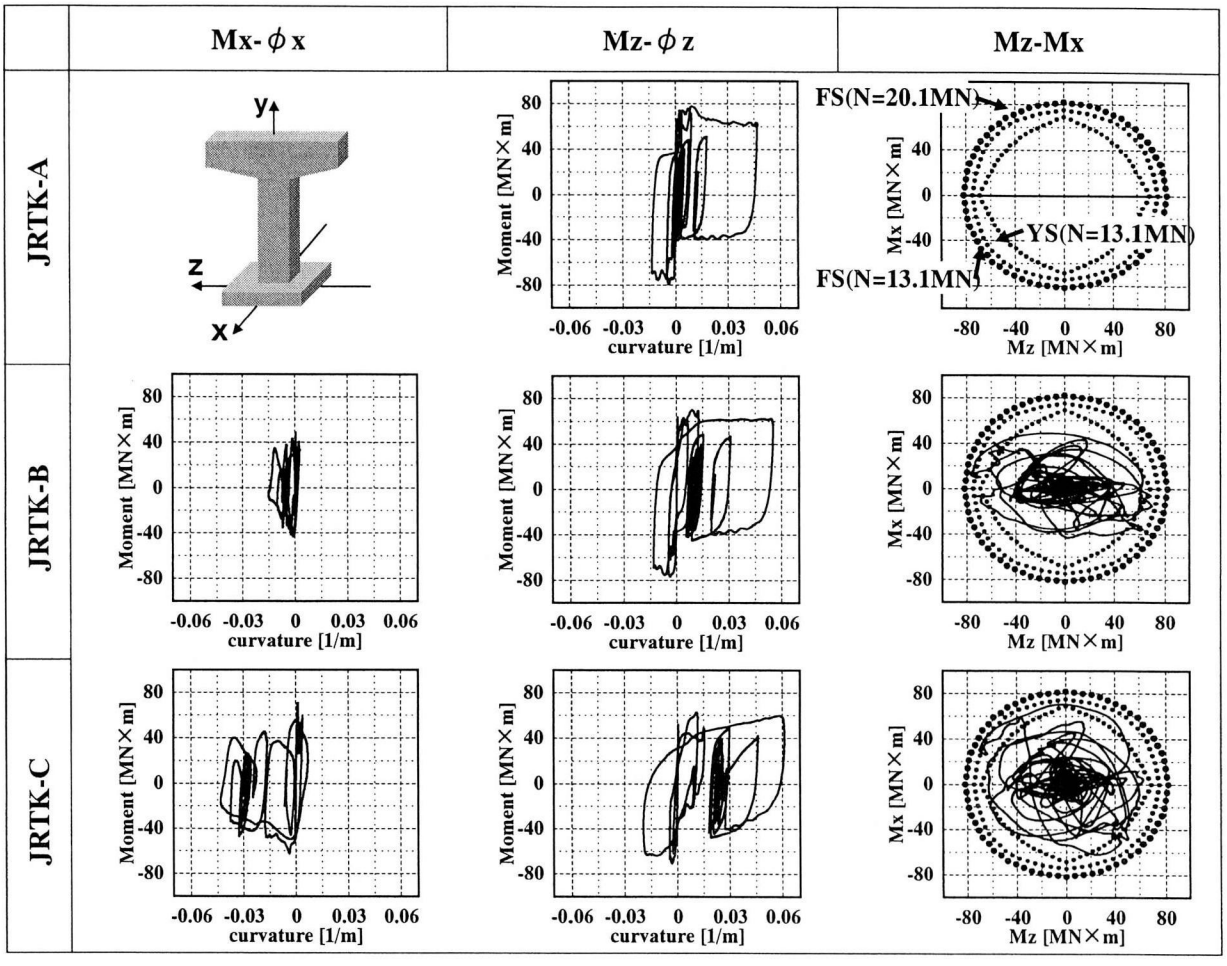

Fig.15 Section hysteresis loops (JRTK)

from 2D-failure points. Therefore the displacement response in x-direction of JMA based on 3-D analysis (JMA-C) is similar to that of 2-D analysis (JMA-A). These contact points with failure surface can explain the reason why the displacement responses of JMA-A to JMA-C (Fig.12) are similar.

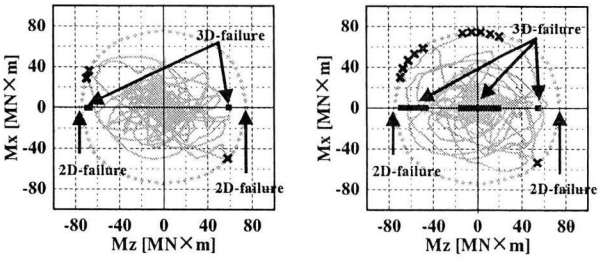

a) JMA-C b) JRTK-C

Fig.16 Projection of 3D-failure points

5. Conclusions

In this paper, numerical evaluation of static and dynamic behavior under bi-axial bending based on application of flexibility method and fiber-model to RC columns for 3-dimensional analysis were carried out. Further, the possibility of degradation of degree-of-freedoms and the explication of this phenomenon were discussed. The results of this study are summarized as follows:

1) The comparisons between the predicted and experimental results of the bi-axial column test show that the flexibility method can reasonably describe the behavior of RC analysis under bi-axial bending.
2) The causes of increment of deflection in fixed loaded direction are composed of steel yielding and concrete crack opening. These two different mechanisms make the stiffness in fixed loaded direction degrade. Therefore, the extension of the 2-D analysis cannot explain that of 3-D analysis.
3) In the dynamic analysis under multi directional loading, the resisting force in one direction degrades as the seismic loading in another direction increases. This may be the risky judgement if the judgement is

based on the projection of 2-dimensional analysis.

Although this study explained the basic mechanisms of bi-axial bending and the effect of multi-directional forces, such as the buckling of steels or spalling of concrete were not considered in these analyses. Moreover, the structure for analysis was just one column and above-mentioned results may not represent the real bridge behavior sufficiently. Therefore these elements are necessary to predict the behavior of real structures.

References

1) Takiguchi, K.,Kokusho, S and Okada, K. : "Experiments on Reinforced Concrete Columns Subjected to Bi-axial Bending Moments," *Transactions of the architectural institute of Japan*, AIJ, Vol.229, pp.25-34, 1975 (in Japanese)

2) Sato,Y., Yoshimura,M., and Tsumura,K., : "Displacement Response of R/C Columns Subjected to Bi-Axial Lateral Loads," *Proceedings of the JCI*, Vol.16, No.2, pp.653-658, 1994 (in Japanese)

3) Oide,K., Nakajima,A. and Saiki,I., : "Three Dimensional Dynamic Response Analysis of Bridge Piers by Rigid-Body-Spring Model," *Journal of Structural Mechanics and Earthquake Engineering*, JSCE, No.654,pp.259-270,2000 (in Japanese)

4) Nakano,T.,and Tanabe,T., : "A Study of Influence of the Analytical Model on the Behavior of RC Piers subjected to Bi-Axial Bending," *Journal of Applied Mechanics*, JSCE, pp.509-518, 2002 (in Japanese)

5) CEB : *RC FRAMES UNDER EARTHQUAKE LOADING*, Thomas Telford, pp.50-60, 1996

6) Spacone,E.,Ciampi,V. and Filippou, F.C., : "Mixed Formulation of Nonlinear Beam Finite Element," *Computers & Sciences*, Vol.58,pp.71-83,1996

7) Coleman, J. and Spacone, E., : "Localization Issues in Nonlinear Frame Elements," *Seminar on post-peak behavior of RC structures subjected to seismic loads*, JCI, Vol.1, pp.157-171, 1999.10

8) Nakano,T.,and Tanabe,T., : "Cyclic Analysis of RC Columns by Flexibility Method," *Transactions of JCI*, Japan Concrete Institute, Vol.23, pp.287-294, 2002

9) Nakano.T.,and Tanabe,T., : "Study on Cyclically and Bi-Axially Loaded RC Columns based on Flexibility Method," JSCE Chubu-branch, pp.507-508, 2002.1

10) Darwin,D.,Pecknold,D.A., : "Analysis of Cyclic Loading of Plane R/C Structures," *Computers & Structures*,Vol.7, pp.137-147, 1977

11) CEB : *RC ELEMENTS UNDER CYCLIC LOADING*, Thomas Telford, pp.58-69, 1996

12) Special Committee on Earthquake Disaster Measures, : *Specifications for Highway Bridges Part V : Seismic Design*, Japan Road Association, 1996 (in Japanese)

13) Wilson, E.L. and Penzien, J. : "Evaluation of Orthogonal Damping Matrix," *International Journal for Numerical Methods in Engineering*, Vol.4, pp.5-10, 1972

14) Hoshikuma, J., Kawashima, K. and Nagaya, K. : "A Stress-Strain Model for Reinforced Concrete Columns Confined by Lateral Reinforcement," *Journal of Materials, Concrete Structures and Pavements*, JSCE, No.520,pp.1-11,1995.8 (in Japanese)

15) Watanabe, H., Sakimoto, T., Nitta, A. and Oishi, K. : "The Ultimate Behavior of Reinforced Concrete Columns under Repeated Transverse Load," *Journal of Structural Engineering*, Vol.43A, pp.339-347, 1997 (in Japanese)

(Received September 13,2002)